Probing the Local Structure of Liquid Water by X-ray Absorption Spectroscopy†

Jared D. Smith,‡,§ Christopher D. Cappa,‡,§ Benjamin M. Messer,‡,§ Walter S. Drisdell,‡,§ Ronald C. Cohen,‡ and Richard J. Saykally*,‡,§

Department of Chemistry, University of California, Berkeley, California 94721, and Chemical Sciences Division, Lawrence Berkeley National Laboratory, Berkeley, California 94721

Received: June 12, 2006; In Final Form: July 14, 2006

It was recently suggested that liquid water primarily comprises hydrogen-bonded rings and chains, as opposed to the traditionally accepted locally tetrahedral structure (Wernet et al. *Science* **2004**, *304*, 995). This controversial conclusion was primarily based on comparison between experimental and calculated X-ray absorption spectra (XAS) using computer-generated ice-like 11-molecule clusters. Here we present calculations which conclusively show that when hydrogen-bonding configurations are chosen randomly, the calculated XAS does not reproduce the experimental XAS regardless of the bonding model employed (i.e., rings and chains vs tetrahedral). Furthermore, we also present an analysis of a recently introduced asymmetric water potential (Soper, A. K. *J. Phys.: Condens. Matter* **2005**, *17*, S3273), which is representative of the rings and chains structure, and make comparisons with the standard SPC/E potential, which represents the locally tetrahedral structure. We find that the calculated XAS from both potentials is inconsistent with the experimental XAS. However, we also show the calculated electric field distribution from the rings and chains structure is strongly bimodal and highly inconsistent with the experimental Raman spectrum, thus casting serious doubt on the validity of the rings and chains model for liquid water.

1. Introduction

The unusual properties of liquid water are thought to result from its unique hydrogen-bonding (HB) network, traditionally viewed as being locally tetrahedral, wherein each water molecule forms ∼4 H bonds (two acceptors and two donors) with nearest neighbors. The HB structure of liquid water was first described as locally tetrahedral in 1933 by Bernal and Fowler,[1] who inferred this type of structure on the basis of water's X-ray diffraction pattern. Since then, numerous other experimental and theoretical methods have supported this type of structure.[2,3] However, this time-honored picture has recently been challenged in favor of a structure in which most molecules (∼80%) form only two H bonds (one acceptor and one donor). In this purposed structure, water molecule would be linked in somewhat of an end-to-end pattern (similar to HF or methanol) and thus strongly favor the formation of hydrogen-bonded rings and chains.[4] It is currently unclear whether such a "ring and chain" model can account for any of water's unusual thermodynamic properties. For instance, the well-known temperature of maximum density is thought to be a consequence of the open nature of its quasi-tetrahedral network structure. In fact, a density maximum appears to be a general characteristic of *tetrahedrally* coordinated liquids[5] and has not been found in liquids known to form only two H bonds per molecule (e.g., HF or methanol). Furthermore, the coordination number for water, derived from the area under the first peak in the O−O radial distribution function (RDF), is ∼ 4.4,[3] compared with values closer to 2 for HF and methanol.[6] A coordination number near 4 is thought to signify that the local tetrahedral structure found in solid ice, which also has a coordination number near 4, is to some extent preserved in the liquid. The position and temperature dependence of the second peak in the O−O RDF is also thought to evidence a local tetrahedral structure.[7,8] However, a recent analysis of X-ray and neutron difraction data by Soper[9] indicates that the diffraction data may indeed not distinguish between symmetric (tetrahedral) and asymmetric (rings and chains) bonding description of water, whereas, a more recent analysis by Head-Gordon et al.[8] indicates that the X-ray scattering data can indeed distinguish between them and are inconsistent with an asymmetric bonding model. Strong theoretical support for a local tetrahedral structure also comes from simulations using both empirical potentials, fit to diffraction data and thermodynamic properties, as well as ab initio simulations. The underlying physics governing these computational methods is quite different, but they both predict hydrogen bonding in a similar locally tetrahedral structure.[10]

Evidence in favor of a "rings and chains" structure has been claimed from theoretical and experimental X-ray absorption and X-ray Raman spectroscopic studies of the oxygen K-edge of liquid water.[4,11,12] In recent years, X-ray absorption spectroscopy (XAS) has emerged as a new tool for the investigation of the local structure of water and aqueous solutions[4,11−20]. XAS is an atom-specific probe in which a core electron is excited to an unoccupied electronic state. The electronic character of these unoccupied states is very sensitive to the local geometric structure, and therefore XAS can serve as an indirect structural probe. It is clear from both experimental and theoretical evidence that the pre-edge region (∼535 eV) of the XAS is a signature of distorted HB configurations, whereas the post-edge region (∼541 eV) is a signature of stronger "ice-like" configurations.[4,12] However, establishing quantitatively how sensitive the XA spectrum is to HB rearrangements, and the underlying structural

† Part of the special issue "Charles B. Harris Festschrift".

* Corresponding author: e-mail saykally@berkeley.edu.

‡ Department of Chemistry, University of California, Berkeley, California, 94721.

§ Chemical Sciences Division, Lawrence Berkeley National Laboratory, Berkeley, California 94721.

10.1021/jp063661c CCC: $33.50
Published on Web 08/19/2006

implications, is highly debated.[4,18,21,22] The pre-edge feature in the XAS of liquid water is relatively prominent, while the post-edge feature is relatively weak, compared with the XAS of crystalline ice.[4] This observation clearly indicates that the hydrogen-bond network is more distorted in liquid water than in ice, which has long been widely accepted. To further quantify the degree of distortion in liquid water compared with ice, it is necessary to determine how sensitive the XAS spectral features (pre-edge and post-edge) are to structural distortions; that is, it is necessary to develop a HB definition that is applicable to the XAS technique and that can be employed to determine the degree of HB distortion required to produce the observed increase (decrease) in pre-edge (post-edge) intensity. Wernet et al.[4] derived a geometric HB definition using calculated XAS spectra of computer-generated ice-like 11-molecule clusters. This was accomplished by exploring radial and angular distortions to the donor H bonds of the central molecule in the cluster. The central molecule was then categorized as having a "broken" hydrogen bond when a pre-edge feature was observed in the calculated XAS. It was concluded from this analysis that a relatively significant degree of HB distortion is required to lead to a pre-edge feature in the XAS. However, as recently pointed out by Fernandez-Serra and Artacho[23] and also illustrated in the supporting material of ref 4, the pre-edge intensity increases smoothly with HB distortion without exhibiting any obvious feature or discontinuity with which to distinguish a "broken" H bonding configuration. Therefore, the HB cutoff chosen by Wernet et al., based on the appearance of the pre-edge feature, is a rather arbitrary one.

In an attempt to establish an experimental HB criterion, we have previously reported temperature-dependent measurements of the XAS.[18] By performing a van't Hoff analysis of the XAS spectral features, we found that the difference in the average energy between the HB population that generates pre-edge intensity, and that which generates post-edge intensity is 1.5 ± 0.5 kcal/mol. This relatively small energy difference was interpreted as indicating that the molecules that contribute to the pre-edge intensity are only slightly distorted compared with those that contribute to the post-edge intensity. This finding was in stark contrast to the geometric definition put forth by Wernet et al.,[4] which indicated that large distortions are required to give an observable pre-edge. It should be noted that an identical energetic difference (1.5 kcal/mol) is obtained[22] from a Boltzmann analysis of temperature-dependent hydrogen-bonding populations reported by Wernet et al. It has since been shown that this type of van't Hoff temperature dependence is completely consistent with a continuous distribution of HB geometries and energies.[24,25] Furthermore, the existence of distinct spectral features associated with different HB geometries is also consistent with a continuous distribution of HB energies, although this may indicate that the relevant spectroscopic observable is a strongly nonlinear function of intermolecular geometry.[25] Therefore, the value of 1.5 kcal/mol derived from our van't Hoff treatment represents an energetic HB definition specific to the observed XAS spectral features (i.e., pre-edge and post-edge) and does not indicate that water is composed of two distinct types of H bonding structures.

The observed XAS of liquid water is fully consistent with a locally tetrahedral structure if, in fact, only relatively minor distortions from the ice structure in the HB network are required to produce the observed pre-edge intensity. Such behavior is precisely what our van't Hoff analysis suggests, but it is inconsistent with the conclusions of Wernet et al. It was suggested by Nilsson et al.[21] that the total electron yield (TEY) XA spectra, used in this van't Hoff analysis, suffered from nonlinear saturation effects, which could explain the discrepancy with the conclusions of Wernet et al. However, and as we have previously pointed out, the relative intensities of the TEY XAS spectral features (pre-edge and main-edge), used in our van't Hoff analysis, are nearly identical to the saturation-corrected XAS reported by Wernet et al., therefore indicating that saturation effects are most likely relatively minor.[22]

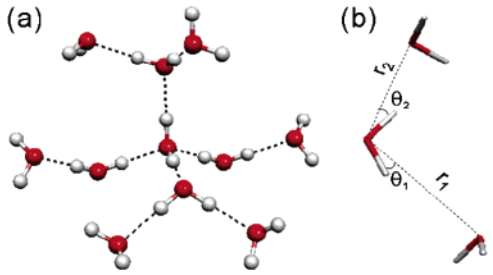

Figure 1. (a) The 11-molecule cluster used to calculate X-ray absorption spectra. (b) XAS was calculated as a function of HB distortion on the donor side by randomly varying the O−O distances (r_1 and r_2) and the corresponding angular deviations from linearity (θ_1 and θ_2).

Another potential explanation for this discrepancy is that the interpretation of Wernet et al. was primarily based on a few calculated XAS spectra on computer-generated ice-like 11-molecule clusters, which may not adequately represent liquid water. To address this possibility, we have performed a series of XAS calculations on a model 11-molecule cluster, very similar to the clusters employed in the analysis of Wernet et al. We have found, using computational methods identical to those described by Wernet et al., that the calculated XAS from a model 11-molecule cluster is not consistent with a water structure comprising a large fraction of "broken" H bonds. Furthermore, we have also calculated the XAS from structures taken from a classical simulation using a standard pair potential (SPC/E), as well as from the asymmetric potential recently introduced by Soper.[9] We find that the calculated XAS of structures derived from both the SPC/E and the Soper potentials cannot quantitatively reproduce the experimental spectrum. We have also calculated the electric (E) field distributions using both of these potentials in order to compare them with the experimental Raman spectrum.[18,26,27] We have found that the E field distribution calculated from the SPC/E potential reproduces the band profile of the experimental spectrum very well, while the asymmetric potential results in a bimodal distribution that is completely inconsistent with experiment.

2. Methods

The oxygen K-edge XAS of liquid water was calculated by use of the StoBe-deMon 2.0 code.[28] StoBe is a commercially available software package based on a density functional theory (DFT) approach for the calculation of XAS. All calculations were performed by the transition-potential method, under the half core hole (HCH) approximation using the nonlocal exchange functional of Becke[29] and the correlation functional of Perdew.[30] The PBE[31] functional was also used for comparison. The oxygen of interest was described with the IGLO−III basis set,[32] and effective core potentials were used on all other oxygen atoms in order to simplify the definition of the core hole.[33] XAS calculations were performed on the central molecules of 11-molecule model clusters (Figure 1). All intramolecular O−H distances were 0.95 Å, and all intramolecular H−O−H angles

were 109.47°. The cluster was initially configured with all O−O distances (r) set to 2.75 Å and with linear H bonds. HB distortions to the central molecule were introduced by randomly moving the nearest neighbors on the hydrogen side (donor side), as well as on the oxygen side (acceptor side). All other non-nearest-neighbor distances and angles were held constant by moving the non-nearest-neighbor molecules in conjunction with the nearest-neighbor molecule they are H-bonded with. The O−O distances (r_1 and r_2) were varied within the range of 2.5−3.9 Å and the O−H−O angles (θ_1 and θ_2) were varied between 0° and ±50° from linearity (see Figure 1B). Each configuration was classified on the basis of the number of donor H bonds formed by the central water molecule [i.e., double donor (DD), single donor (SD), or no donor (ND)]. This classification is based on the HB definition given in ref 4. By this definition, two water molecules are considered bonded if the O−O distance (r_{O-O}) is less than an angular- (θ-) dependent radial cutoff ($r_{O-O} = 3.3\ \text{Å} - 0.00044\theta^2$), where θ refers to the angular deviation from linearity (in degrees). Since the StoBe-DeMon code generates stick spectra, an artificial broadening scheme must be applied in order to compare with experimental spectra. The broadening scheme employed here involves convolution of the calculated spectra with Gaussians of full width at half-maximum (fwhm) of 0.8 eV below 537.5 eV and 8 eV above 550 eV. Between 537.5 and 550 eV, the fwhm is linearly increased from 0.8 to 8 eV. This broadening scheme will be discussed in more detail in the following section. All of the methods described here for the calculation of XA spectra from model 11-molecule clusters are essentially identical to those employed by Wernet et al.[4]

We have also calculated the XAS for configurations taken from a molecular dynamics (MD) simulation using the SPC/E potential. The SPC/E simulation was performed at room temperature and consisted of 864 molecules in a periodically replicated cubic box of length 29.876 Å. We have also performed similar calculations on configurations taken from a simulation using Soper's asymmetric potential.[9] In both of these cases, 30 molecule clusters were taken from snapshots of the respective simulations. For these calculations, a molecule is selected along with its 29 nearest neighbors based on their O−O distance. A total of 60 configurations were randomly chosen from each simulation. We have also calculated the value of the electric (E) field at the position of each H atoms, and projected onto the OH bonds, that is due to all surrounding molecules (and their periodic images) for both the standard SPC/E potential and Soper's asymmetric potential. The distributions of E fields calculated from the simulations are compared with the OH Raman spectrum of HOD in D_2O. The methods we have used to calculated the E field and to measure the Raman spectrum have been described in a previous publication.[24]

3. Results and Discussion

The XAS of liquid water was first interpreted as evidencing a large population (60−80%) of molecules forming only two H bonds by Nilsson and co-workers.[12] This original interpretation used a procedure wherein the bulk ice XAS was subtracted from the liquid water XAS until negative features were observed. While this is already a highly approximate approach for structural determination, their analysis was further complicated by the fact that the measured fluorescent yield XAS suffered from severe saturation effects.[11] Spectral saturation effectively reduces the strongest spectral features relative to weaker features,[17,34] therefore resulting in a water spectrum with artificially enhanced pre-edge intensity (weakest feature) relative to the main-edge (strongest feature). In an unsaturated XA spectrum at room temperature, the pre-edge to main-edge ratio is 0.38−0.40;[22] however, the XAS reported in ref 12 exhibits an artificially enhanced ratio of 0.61. In a second paper by this same group, the X-ray Raman spectrum (XRS) of liquid water was also interpreted as constituting evidence for liquid water structure with greater than 70% highly distorted water molecules (forming only 2 H bonds).[11] In that work, the reported XRS spectrum also showed an artificially enhanced pre-edge to main-edge ratio of 0.54. However, this artifact was a result of nondipole contributions, as opposed to saturation effects, which are not a factor in XRS.[4] More recently Wernet et al.[4] have reported XAS and XRS that were corrected for saturation effects and ostensibly free from nondipole contributions, respectively, resulting in a pre-edge to main-edge ratio of 0.40. Nevertheless, the population of strongly distorted water molecules was again determined to be 80%. That the spectra used in these three studies exhibit dramatically different relative pre-edge intensities (0.40−0.61), and yet each was interpreted as evidencing a large population (60−80%) of molecules with two intact and two "broken" or strongly distorted H bonds, indicates that the spectral analysis employed in these studies is relatively insensitive to the actual details of the spectral features. This is troubling considering that the relative pre-edge intensity is the primary signature of distorted species in these K-shell spectra.[4]

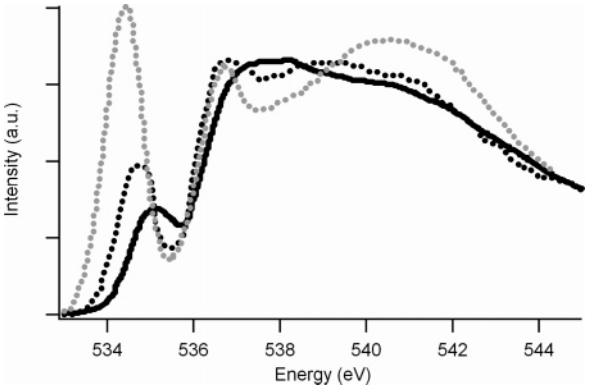

Figure 2. Direct comparison of the ice surface spectrum (dotted black line) and the bulk water spectrum (solid line) reported in ref 4. The TIY ice surface spectrum (dotted gray line) measured by Parent et al.[35] The considerably stronger pre-edge in both ice surface spectra indicates that the fraction of single donor molecules at the ice surface (50−80%) is larger than in liquid water.

It has also been suggested that the close resemblance of the ice surface spectrum to the bulk water spectrum indicates that the majority of water molecules in the liquid are in a similar bonding situation as those at the ice surface.[4] However, there are several deficiencies in this analysis. For one, when the ice surface XAS and the bulk water XAS are directly compared, it is found that they are actually quite dissimilar. Figure 2 compares the surface ice spectrum to the bulk water spectrum as reported in ref 4. It is clearly seen that the pre-edge in the ice surface spectrum is much stronger than the pre-edge in bulk water and is shifted to lower energy. Therefore, this comparison indicates that the population of distorted species in liquid water is at most *less* than that at the ice surface (50−80%). Furthermore, the highly surface-sensitive total ion yield (TIY) spectrum of ice reported by Parent et al.[35] (also shown in Figure 2) has a much stronger pre-edge feature than the ice surface spectrum reported by Wernet et al. This difference may result from the fact that the ice surface XAS measured by Wernet et al. is not directly experimentally observed but is actually a difference spectrum generated by subtracting 60% of the normal

incidence Auger electron yield (AEY) X-ray spectrum from the grazing incidence AEY spectrum (i.e., [grazing AEY] − 0.6-[normal AEY]).[4] This method assumes that the electron escape depths for theses two methods (grazing and normal AEY) are accurately known, which may not be the case.

As discussed in the Introduction, another spectral comparison cited as evidence for a "rings and chains" structure is that between the bulk ice XAS and liquid water XAS.[4] The XAS of bulk ice has a very weak pre-edge feature and a relatively strong post-edge feature compared to those of liquid water. This has been interpreted by Nilsson and co-workers as indicating that liquid water lacks the local tetrahedral structure present in ordinary ice. However, as mentioned previously, with no a priori knowledge of the XAS/XRS spectral response to geometric distortion, such a comparison indicates the obvious fact that the degree of HB distortion in liquid water is greater than that in ice. In other words, for such a comparison to be meaningful, it is necessary to quantify precisely how sensitive XAS/XRS spectral features are to distortions in the HB network.[18] *Therefore, and despite the claims of Nilsson and co-workers,*[4,17,36] *comparison of the XAS of liquid water to the XAS of the bulk and surface of ice does not in and of itself indicate that liquid water forms only two H bonds.* In fact, such a comparison only indicates that the degree of HB distortion in liquid water lies somewhere between that of bulk ice and the ice surface, which is entirely consistent with the standard interpretation of liquid water's HB structure. To make more definitive claims about HB structure from the XAS/XRS data, it is necessary to compare against spectral calculations on model structures. Therefore, the current evidence for a liquid water structure with only two H bonds comes *exclusively* from the comparison with density functional theory-based XA spectral calculations.

The preceding discussion demonstrates that a comparison of the liquid water XAS with those of bulk ice and the ice surface cannot establish the degree of HB distortion in water, and it is therefore necessary to develop a working HB definition consistent with the XAS technique.[18] The geometric HB definition put forward by Wernet et al. from XAS calculations on 11-molecule ice-like clusters was used to classify 14 model configurations into separate H bonding categories based on the number of donor H-bonds (i.e., SD, DD, or ND). The experimental XRS was then fit by use of the XAS calculated from these 14 configurations. The best fit to experiment was achieved with the relative weights of 80% SD, 15% DD, and 5% ND. This type of analysis necessarily assumes that the calculated spectra are rigorously correct and that the structures used in them are representative of the equilibrated liquid. However, we have found that there is a very large degree of variation in the individual calculated K-shell spectra even for clusters with similar H-bonding configurations within the same class (SD, DD, etc.). Therefore, the limited sampling of configurations considered by Wernet et al. (5 DDs, 8 SDs, and 1 ND) were probably inadequate to produce a spectrum representative of the high degree of disorder that exists in a liquid.

To generate a XAS that is more representative of room-temperature liquid water, we have performed spectral calculations on 150 total configurations (60 SD, 60 DD, and 30 ND) using the same 11-molecule cluster as Wernet et al. The large variation in the calculated spectra is evident in Figure 3, which shows the XA spectra calculated from five slightly different SD configurations. In fact, we have found that ∼25% of the calculated SD spectra actually exhibit little or no pre-edge intensity (see Figure 3c,e for examples). Furthermore, we have

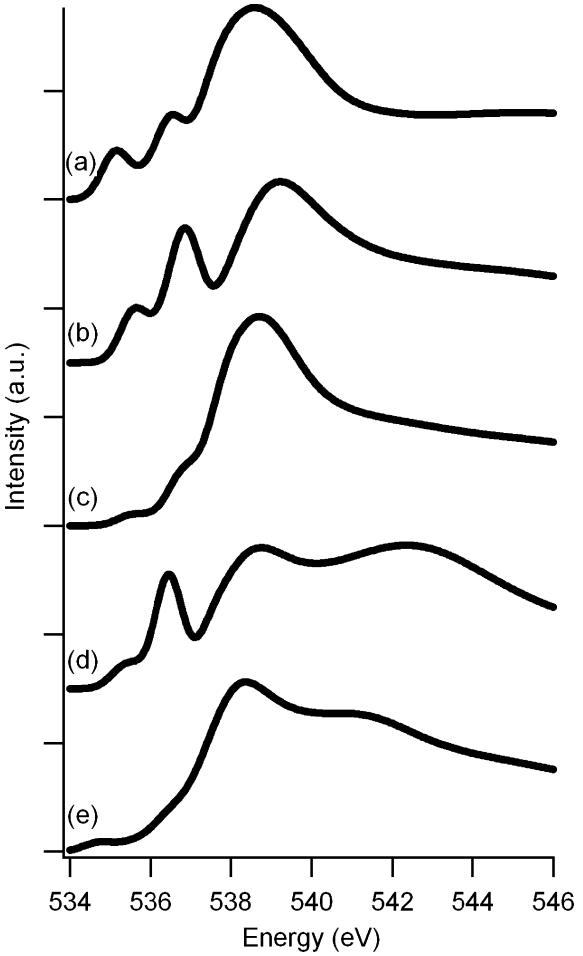

Figure 3. Calculated XAS vary significantly even among HB species defined as single donor. Comparison of calculated spectra from 11-molecule clusters in five different SD configurations (as defined by Wernet et al.[4]) with similar geometries. The donor-side HB geometries of theses configurations correspond to (a) $r_1 = 2.9$ Å, $\theta_1 = -47.3°$, $r_2 = 2.7$ Å, $\theta_2 = 28.6°$; (b) $r_1 = 3.6$ Å, $\theta_1 = 44.3°$, $r_2 = 2.6$ Å, $\theta_2 = 37.5°$; (c) $r_1 = 3.7$ Å, $\theta_1 = 33.1°$, $r_2 = 2.5$ Å, $\theta_2 = -39.3°$; (d) $r_1 = 3.8$ Å, $\theta_1 = 32.2°$, $r_2 = 2.6$ Å, $\theta_2 = 0.9°$; (e) $r_1 = 3.1$ Å, $\theta_1 = 21.2°$, $r_2 = 2.6$ Å, $\theta_2 = -22.4°$.

also found that a similar fraction of DD species *do* show a clear pre-edge feature. The fact that a number of spectra calculated from DD species show a pre-edge while a number of SD spectra do not show a pre-edge indicates that the use of a geometric HB definition based on the occurrence of an XAS pre-edge feature is, in fact, quite arbitrary. We have nonetheless attempted to reproduce the experimental water spectrum by weighting the average calculated spectrum in the same manner as did Wernet et al. (SD:DD:ND = 85:10:5), as well as by employing a weighting scheme more consistent with a traditional locally tetrahedral structure (SD:DD:ND = 15:85:5) (Figure 4). It is immediately apparent from Figure 4 that neither weighting scheme quantitatively reproduces the experimental spectrum. This is in disagreement with the weighted XAS calculated by Wernet et al. from only 14 individual cluster configurations, which reproduced the experimental spectrum remarkably well. It should be noted that we have confirmed that our computational methods are nearly identical to those employed by Wernet et al. by reproducing the various calculated XAS shown in Figure 3A of ref 4. Furthermore, if we randomly pick only 14 configurations, we still are unable to reproduce the experimental spectrum. In fact, we have found that in order to reproduce the experimental spectrum, it is necessary to choose clusters with

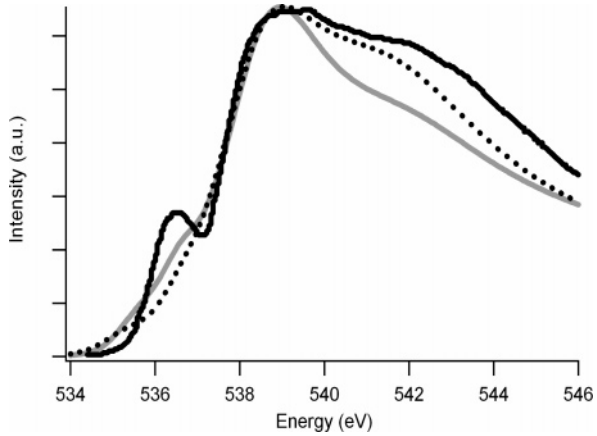

Figure 4. Direct comparison of the calculated XAS by use of the Wernet et al.[4] relative weights of SD:DD:ND = 85:10:5 (solid gray line), and the locally tetrahedral weights SD:DD:ND = 10:85:5 (dotted black line), with the experimental spectrum reported in ref 4 (solid black line). The experimental spectrum has been shifted by ~1.4 eV and the intensity has been scaled for comparison with the calculated spectra.

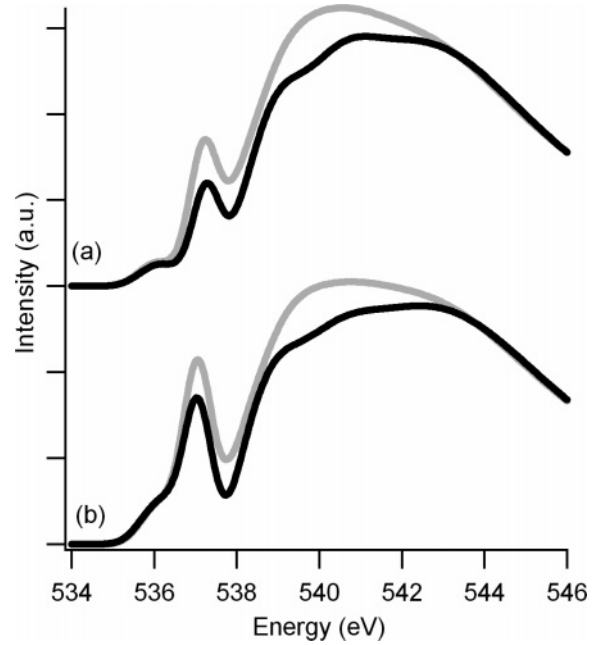

Figure 5. Dependence of calculated XAS on the density functional used. XAS calculated by use of the exchange and correlation functional of Becke[29] and Perdew[30] (gray) was compared to XAS calculated by use of the PBE[31] functional (black) for two different H bonding configurations. It was necessary to shift the calculated XAS, from the PBE functional, by 0.85 eV for comparison. The donor side HB geometries of theses configurations correspond to (a) $r_1 = 3.5$ Å, $\theta_1 = 0°$, $r_2 = 2.75$ Å, and $\theta_2 = 0°$ or (b) $r_1 = 3.5$ Å, $\theta_1 = 35°$, $r_2 = 2.75$ Å, and $\theta_2 = 0°$.

very specific H bonding configurations, that is, those in which the individual calculated XAS already exhibit good agreement with experiment.

Reproducing the experimental XA spectrum in such a manner is further complicated by the strong density functional dependence of the calculated XAS (Figure 5). Use of the PBE[31] functional, which has been shown to satisfactorily reproduce the RDF for water[37] and has recently been used for the calculation of XAS,[38,39] tends to increase the intensity in the post-edge region relative to the main-edge. Another potential complication with these calculations is that since the StoBe code yields only the positions and oscillator strengths of K-shell

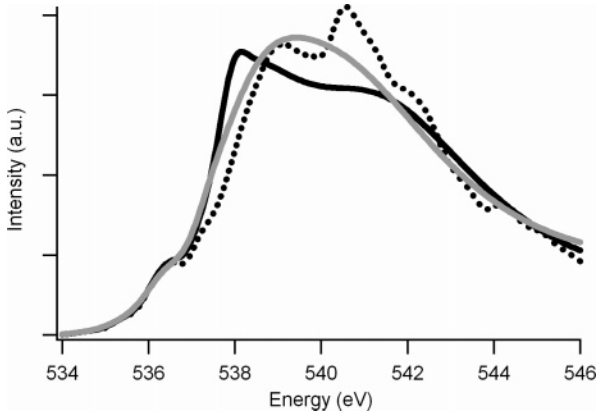

Figure 6. Calculated XAS vary significantly with the spectral broadening scheme used. The average calculated XAS from 60 SPC/E configurations by use of three different previously reported broadening schemes are compared. The dotted black line uses a constant broadening of 0.5 eV, the solid black line uses a linearly increasing broadening scheme reported by Cappa et al.,[13] and the solid gray line uses the linearly increasing scheme reported by Wernet et al.[4] The scheme reported by Cappa et al. most resembles the experimental spectrum.

transitions, an arbitrary broadening scheme must be chosen, and this choice has a dramatic effect on the calculated spectrum. We will discuss this broadening scheme in more detail shortly. Therefore, considering that randomly chosen HB configurations cannot reproduce the experimental spectrum (regardless of the weighting scheme employed), as well as the large functional and broadening scheme dependence, we find that XAS calculations from model clusters cannot provide unambiguous support for the "rings and chains" model purposed by Wernet et al. On the contrary, we have found that XAS calculations on model 11-molecule clusters are unable to quantitatively reproduce the experimental spectrum, most likely due to the approximations inherent in the half core hole DFT approach for spectral calculations, the necessity of using an arbitrary spectral broadening scheme, and the use of small clusters, which do not adequately represent the liquid.

All of the calculations presented thus far were performed on ideal 11-molecule clusters, which were unable to reproduce the experimental XAS. As a more realistic model system, we have performed calculations on 30-molecule clusters taken from a SPC/E MD snapshot. The SPC/E potential, which exhibits locally tetrahedral intermolecular arrangements, has been shown to satisfactorily reproduce the X-ray scattering data for liquid water[40] as well as the HB energetics derived from Raman measurements.[24] As previously mentioned, another potential complication related to calculating XAS is that an arbitrary broadening scheme must be chosen in order to compare calculated XAS with experiment. Typically the calculated spectrum is convoluted with a constant Gaussian line shape with a width of 0.3,[39] 0.5,[41] or 0.6[38] eV. Broadening schemes in which the Gaussian width is linearly increased across the spectrum have also been employed.[4,13,41] We have found that the chosen broadening scheme can have a dramatic effect on the calculated spectrum. Figure 6 shows the average calculated XAS from 60 randomly chosen SPC/E configurations and broadened by use of three different previously reported schemes. It appears that the broadening scheme employed by Cappa et al.[13] most resembles the experimental spectrum. However, all of these schemes are nevertheless arbitrary and have no firm theoretical foundations. Wernet et al. chose their broadening scheme by fitting the calculated ice spectrum to the experimental ice spectrum. However, we have calculated the XAS from a 31-molecule hexagonal ice cluster[42] and have found that the

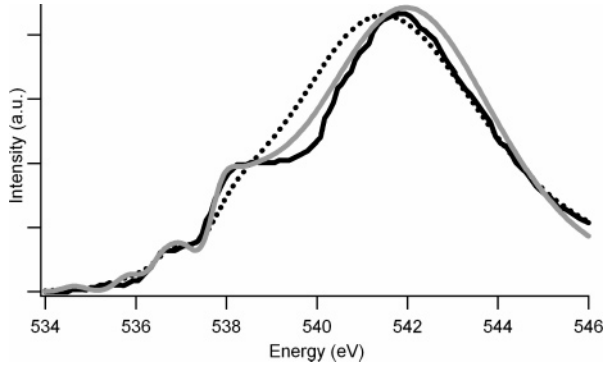

Figure 7. Direct comparison of the calculated ice XAS by use of the broadening scheme of Cappa et al.[13] (solid gray line) and the broadening scheme of Wernet et al.[4] (dotted black line) and the experimental ice spectrum reported in ref 4 (solid black line). The experimental spectrum has been shifted by ~1.7 eV and the intensity has been scaled for better comparison with calculated spectra.

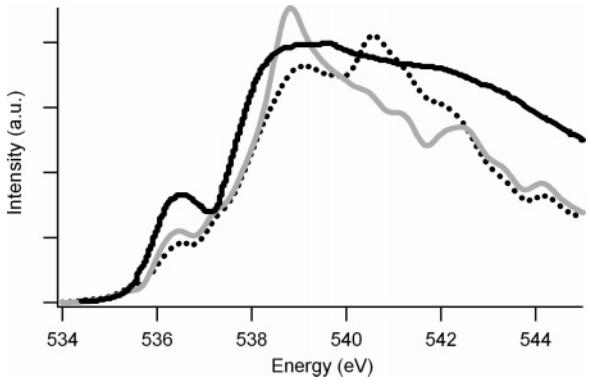

Figure 8. Direct comparison of the average calculated XAS from 60 SPC/E configurations with the experimental XAS reported in ref 4 (solid black line). The dotted black line is the direct average of the 60 randomly chosen SPC/E configurations, and the solid gray line is the weighted average (SD:DD:ND = 85:10:5). A constant 0.5 eV broadening has been used. The experimental spectrum has been shifted by ~1.4 eV and the intensity has been scaled for better comparison with calculated spectra.

broadening scheme employed by Cappa et al. does similarly well in reproducing the experimental ice spectrum from ref 4 (Figure 7). Therefore, fitting to experiment does not uniquely establish a "correct" broadening scheme.

To minimize the ambiguity associated with the use of these broadening schemes, in subsequent calculations we use a constant width of 0.5 eV. However, we note that the use of a constant broadening ignores the increase in lifetime broadening found above the ionization edge. Figure 8 shows the average calculated XAS from 60 randomly chosen SPC/E configurations (37 DDs, 21 SDs, and 2 NDs) compared with a weighted average (SD:DD:ND = 85:10:5) calculated from the same configurations. As is the case with the ideal 11-molecule cluster, neither calculated spectrum accurately reproduces the experimental XAS. The poor agreement between experimental and calculated spectra shown in Figure 8 could result from two sources: (1) The DFT-based XAS calculations using the half core hole (HCH) approximation, and the associated broadening scheme are not sufficiently accurate to quantitatively reproduce the experimental spectrum, or (2) the molecular structures (both the simple and the weighted average) employed in these calculations are not representative of the actual liquid water structure. Strong evidence for the first possibility was recently reported by Prendergast and Galli,[39] wherein it was shown that XAS spectral calculations, employing the excited state core hole (XCH) method, are able to reasonably reproduce the experimental water spectrum by use of structures from the TIP4P classical potential (which yields a locally tetrahedral structure similar to that of the SPC/E potential). This may indicate that the use of the HCH approximation is not appropriate for quantitative interpretation of XAS calculations of a highly disordered system like liquid water, which has been a subject of ongoing debate.[36,38] In contrast, Odelius et al.[41] have claimed that the poor agreement with experiment of HCH XAS calculations on structures generated from a classical and ab initio simulation indicates that the familiar picture of water as being a locally tetrahedral liquid is incorrect. It was further shown in this work that the average calculated XAS from only the SD configurations in the simulation similarly does not agree with experiment. To force approximate agreement of the calculated and experimental XAS, Odelius et al. developed a more stringent HB definition, which included a 0.8 Å exclusion zone. Here, every molecule was considered to have one strong HB with an O−O distance less than 2.9 Å, and one highly distorted HB with an O−O distance greater than 3.7 Å, and O−O distances between 2.9 and 3.7 Å were excluded. However, this HB definition essentially constitutes a two-state model wherein H bonds can be either very strong or very weak, with none being intermediate. Recent experimental and theoretical evidence strongly suggests that the H bond geometries in liquid water are continuous[24,25,43] and therefore that such a two-state model is not an accurate description of the intermolecular geometries in liquid water. Therefore, it appears that DFT-based XAS calculations, employing the HCH approximation, are not sufficiently accurate to *quantitatively* reproduce the experimental water spectrum. This conclusion is based on the fact that XAS calculations, by the XCH method of Prendergast and Giulia,[39] reproduce the experimental spectrum from a standard locally tetrahedral structure and that a rather unrealistic two-state model must be invoked for the HCH method in order to give even approximate agreement with the experiment. However, based on the results shown in Figure 6, the degree to which calculation and experiment agree (or fail to agree) will depend importantly on the details of the broadening scheme used. On the other hand, XAS calculations with the HCH approximation do satisfactorily reproduce experimental spectra of crystalline solids[4] and adsorbed species on metal substrates.[44] Furthermore, a number of studies have also shown that this type of calculation can reproduce some of the general aspects of the observed spectral changes resulting from the addition of solutes,[13,15,45] and can therefore serve as a very useful tool for a *qualitative* spectral analysis. However, a *quantitative* analysis, such as that of Nilsson and co-workers, in which the fraction of a specific type of H bonding configuration in a disordered liquid is specified, appears to be beyond the capabilities of these rather approximate methods.

As a final test of this conclusion, we have also performed XAS calculations on structures generated by use of Soper's asymmetric potential.[9] In this potential, a partial charge is placed on only one of the two H atom sites, resulting in an asymmetric bonding situation wherein each water molecule forms only two H bonds.[9] The average calculated XAS from 60 randomly chosen asymmetric configurations with a constant 0.5 eV broadening is shown in Figure 9. Although there is indeed more intensity in the pre-edge region, the overall agreement with experiment is still quite poor. Given the poor agreement with experiment for both the standard SPC/E potential and the asymmetric potential, the calculated XAS can therefore not distinguish which type of HB structure actually best represents

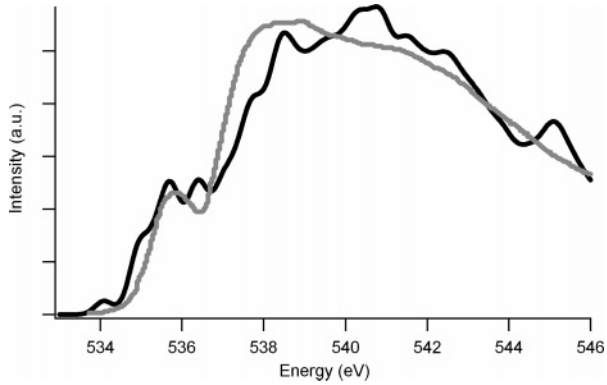

Figure 9. Comparison of the average calculated XAS from 60 asymmetric configurations (black line), generated by use of Soper's asymmetric potential,[9] with the experimental XAS reported in ref 4 (gray line). A constant 0.5 eV broadening has been used. The experimental spectrum has been shifted by ~0.7 eV and the intensity has been scaled for better comparison with calculated spectra.

the correct liquid water structure. As a second comparison of these two potentials, we have calculated the electric (*E*) fields exerted on the H atoms by all surrounding molecules projected on the OH bond. It has been shown that the inhomogeneous broadening of the OH vibrational frequency of HOD in D_2O is directly proportional to the corresponding *E* field experienced by the H atom.[24,26,27] Therefore, if it is assumed that the transition moment is independent of frequency, which is a good approximation for the Raman spectrum,[27] then the shape of the *E* field distribution calculated from a simulation should closely approximate the shape of the experimental HOD spectrum, assuming that the simulated liquid structure is correct. This approximation ignores dynamic effects (i.e., motional narrowing), and therefore assumes that inhomogeneous broadening determines the basic line shape. Figure 10 shows a comparison of the experimental Raman spectrum with the *E* field distribution calculated from the asymmetric potential and from the standard SPC/E potential. It should be noted that the asymmetric *E* field distribution (Figure 10A) is slightly noisier because it was not calculated over an entire trajectory but instead from only 10 statistically independent snapshots. Nonetheless, it is clear from Figure 10 that the shape of the *E* field distribution calculated from an SPC/E simulation reproduces the band profile of the experimental Raman spectrum remarkably well but that the distribution calculated from the asymmetric potential shows a strongly bimodal distribution that is incompatible with experiment. We note that since the *E* field is linearly related to OH vibrational frequency,[26,27,43] converting from *E* field to vibrational frequency will not change the shape of the *E* field distributions shown in Figure 10. The bimodal structure clearly indicates that an asymmetric distribution of charge leads to a highly unrealistic *E* field distribution that is inconsistent with experiment. Furthermore, the OH vibrational frequency has been shown to be primarily determined by the *E* field produced by its H bonding partner (i.e., the HB acceptor).[26,43] Therefore, the two distinct features in the asymmetric *E* field distribution most likely reflect the H bonding disparities between the H atom with a partial charge and the H atom without.

We thus find compelling evidence from several different arguments contravening the validity of the "rings and chains" model for the hydrogen-bonding structure of liquid water, in agreement with several recent papers by other groups.[8,23,39] On the other hand, the recent advances made in experimental measurement of core-excited spectra of liquids with third-generation X-ray light sources still hold the promise of becoming

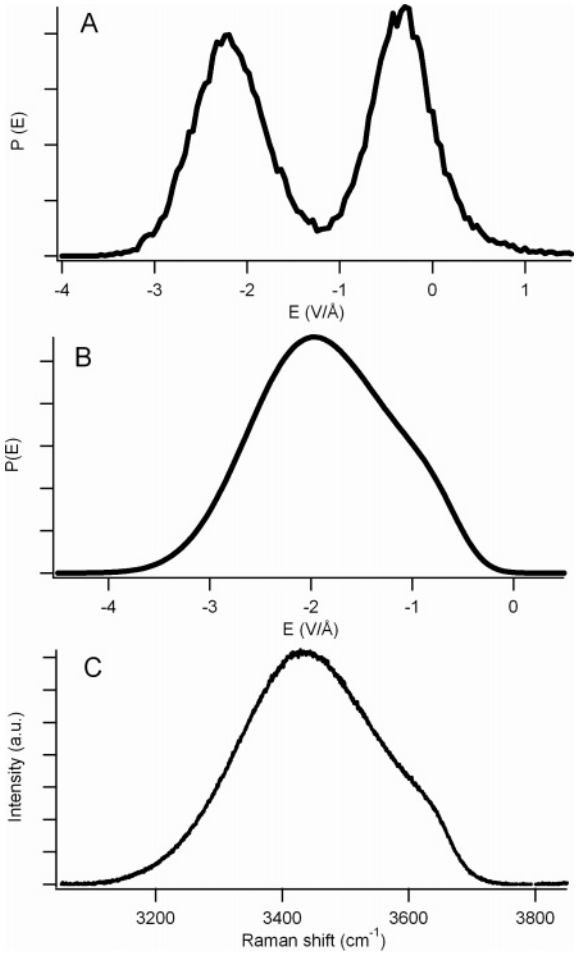

Figure 10. *E* field distribution calculated from an asymmetric potential (panel A) and the standard SPC/E potential (panel B). The experimental OH Raman spectrum of HOD in D_2O is shown for comparison (panel C). The shape of the *E* field distributions from the symmetric SPC/E potential clearly shows much better agreement with the experimental Raman spectrum.

a powerful new tool for probing the structure of liquids. However, exactly what new information can be extracted from these experiments is still not established. It seems apparent that the combination of ab initio calculations of K-shell spectra of clusters derived from snapshots of equilibrated liquid simulations with these new experiments can provide important new *qualitative* insights into the nature of solvent structure in pure liquids, as well as the solvation shells of solutes in solutions. However, it is also clear that further advances in the computation of core-excitation spectra of disordered systems will be necessary for *quantitative* conclusions to be drawn from X-ray data. Given the rapid development of third- and fourth-generation synchrotrons, it would seem that such theoretical developments would merit high priority.

4. Conclusions

We have performed O K-shell XA spectral calculations on model 11-molecule clusters using methods identical to those previously reported by Wernet et al.[4] In contrast to this previous study, we have found that when randomly chosen H bonding configurations are considered, the average calculated XAS does not reproduce the experimental XAS or XRS spectra. This finding is independent of what types of H bonding configurations are used in the average (i.e., SD:DD:ND = 85:10:5 vs SD:DD:ND = 15:85:5). We also conclude that this type of

analysis is further complicated by the density functional dependence of the calculated XAS as well as by the dependence on the arbitrarily chosen spectral broadening scheme. We have also performed calculations on structures generated from a classical simulation using both an asymmetric potential, representative of the "rings and chains" structure of the liquid proposed by Nilsson et al., and with the standard SPC/E potential. We have found that the calculated XAS for structures generated from either potential do not quantitatively reproduce the experimental XAS. However, we have calculated the distribution of *E* fields for both potentials and compared them with the experimental Raman spectrum. We have found the distribution from the asymmetric distribution is strongly bimodal, in direct contrast to both the unimodal SPC/E distribution and the familiar experimental Raman spectrum. In summary, we conclude that while comparisons between calculated and measured XAS or XRS can clearly provide useful new *qualitative* insights into the nature of liquid structure, the state of the theoretical models is insufficiently developed to justify a *quantitative* analysis, such as that advocated by Nilsson and co-workers,[11,12,19,41] particularly given that their proposed conclusions entail overturning more than 50 years of study into the nature of liquid water.

Acknowledgment. This work was supported by the Chemical Sciences, Geosciences, and Biosciences Division of the U.S. Department of Energy. XAS calculations were performed at the U.C. Berkeley College of Chemistry Molecular Graphics and Computation Facility (NSF Grant No. CHE-0232882). CDC was supported by the Advanced Light Source Doctoral Fellowship in Residence and the National Defense Science and Engineering Graduate Fellowship. We thank Dr. Alan Soper for providing the asymmetric snapshots and Professor Phillip Geissler for the SPC/E snapshots.

References and Notes

(1) Bernal, J. D.; Fowler, R. H. *J. Chem. Phys.* **1933**, *1*, 515.

(2) Eisenberg, D.; Kauzmann, W. *The Structure and Properties of Water*; Oxford University Press: New York, 1969.

(3) *The Physics and Physical Chemistry of Water*; Franks, F., Ed.; Plenum Press: New York, 1972; Vol. 1.

(4) Wernet, P.; Nordlund, D.; Bergmann, U.; Cavalleri, M.; Odelius, M.; Ogasawara, H.; Naslund, L. A.; Hirsch, T. K.; Ojamae, L.; Glatzel, P.; Pettersson, L. G. M.; Nilsson, A. *Science* **2004**, *304*, 995.

(5) Angell, C. A.; Bressel, R. D.; Hemmati, M.; Sare, E. J.; Tucker, J. C. *Phys. Chem. Chem. Phys.* **2000**, *2*, 1559.

(6) Garberoglio, G.; Pasqualini, D.; Sutmann, G.; Vallauri, R. *J. Mol. Liq.* **2002**, *96*−*7*, 19.

(7) Hura, G.; Russo, D.; Glaeser, R. M.; Head-Gordon, T.; Krack, M.; Parrinello, M. *Phys. Chem. Chem. Phys.* **2003**, *5*, 1981.

(8) Head-Gordon, T.; Johnson, M. *Proc. Natl. Acad. Sci. U.S.A.* **2005**, *103*, 7973.

(9) Soper, A. K. *J, Phys.: Condens. Matter* **2005**, *17*, S3273.

(10) Mantz, Y. A.; Chen, B.; Martyna, G. J. *J. Phys. Chem. B* **2006** (in press).

(11) Bergmann, U.; Wernet, P.; Glatzel, P.; Cavalleri, M.; Pettersson, L. G. M.; Nilsson, A.; Cramer, S. P. *Phys. Rev. B* **2002**, *66*.

(12) Myneni, S.; Luo, Y.; Naslund, L. A.; Cavalleri, M.; Ojamae, L.; Ogasawara, H.; Pelmenschikov, A.; Wernet, P.; Vaterlein, P.; Heske, C.; Hussain, Z.; Pettersson, L. G. M.; Nilsson, A. *J. Phys.: Condens. Matter* **2002**, *14*, L213.

(13) Cappa, C. D.; Smith, J. D.; Wilson, K. R.; Messer, B. M.; Gilles, M. K.; Cohen, R. C.; Saykally, R. J. *J. Phys. Chem. B* **2005**, *109*, 7046.

(14) Cavalleri, M.; Ogasawara, H.; Pettersson, L. G. M.; Nilsson, A. *Chem. Phys. Lett.* **2002**, *364*, 363.

(15) Messer, B. M.; Cappa, C. D.; Smith, J. D.; Drisdell, W. S.; Schwartz, C. P.; Cohen, R. C.; Saykally, R. J. *J. Phys. Chem. B* **2005**, *109*, 21640.

(16) Messer, B. M.; Cappa, C. D.; Smith, J. D.; Wilson, K. R.; Gilles, M. K.; Cohen, R. C.; Saykally, R. J. *J. Phys. Chem. B* **2005**, *109*, 5375.

(17) Naslund, L. A.; Edwards, D. C.; Wernet, P.; Bergmann, U.; Ogasawara, H.; Pettersson, L. G. M.; Myneni, S.; Nilsson, A. *J. Phys. Chem. A* **2005**, *109*, 5995.

(18) Smith, J. D.; Cappa, C. D.; Wilson, K. R.; Messer, B. M.; Cohen, R. C.; Saykally, R. J. *Science* **2004**, *306*, 851.

(19) Wernet, P.; Testemale, D.; Hazemann, J. L.; Argoud, R.; Glatzel, P.; Pettersson, L. G. M.; Nilsson, A.; Bergmann, U. *J. Chem. Phys.* **2005**, *123*, 154503.

(20) Wilson, K. R.; Rude, B. S.; Smith, J.; Cappa, C.; Co, D. T.; Schaller, R. D.; Larsson, M.; Catalano, T.; Saykally, R. J. *Rev. Sci. Instrum.* **2004**, *75*, 725.

(21) Nilsson, A.; Wernet, P.; Nordlund, D.; Bergmann, U.; Cavalleri, M.; Odelius, M.; Ogasawara, H.; Naslund, L. A.; Hirsch, T. K.; Glatzel, P.; Pettersson, L. G. M. *Science* **2005**, *308*.

(22) Smith, J. D.; Cappa, C. D.; Messer, B. M.; Cohen, R. C.; Saykally, R. J. *Science* **2005**, *308*.

(23) Fernandez-Serra, M. V.; Artacho, E. *Phys. Rev. Lett.* **2006**, *96*, 0164040.

(24) Smith, J. D.; Cappa, C. D.; Wilson, K. R.; Cohen, R. C.; Geissler, P. L.; Saykally, R. J. *Proc. Natl. Acad. Sci. U.S.A.* **2005**, *102*, 14171.

(25) Geissler, P. L. *J. Am. Chem. Soc.* **2005**, *127*, 14930.

(26) Fecko, C. J.; Eaves, J. D.; Loparo, J. J.; Tokmakoff, A.; Geissler, P. L. *Science* **2003**, *301*, 1698.

(27) Corcelli, S. A.; Skinner, J. L. *J. Phys. Chem. A* **2005**, *109*, 6154.

(28) Hermann, K.; Pettersson, L. G. M.; Casida, M. E.; Daul, C.; Goursot, A.; Koester, A.; Proynov, E.; St-Amant, A.; Salahub, D. R.; Carravetta, V.; Duarte, H.; Godbout, N.; Guan, J.; Jamorski, C.; Leboeuf, M.; Malkin, V.; Malkina, O.; Nyberg, M.; Pedocchi, L.; Sim, F.; Triguero, L.; Vela, A. StoBe-deMon v. 2.0, StoBe Software, 2004; available at http://w3.rz-berlin.mpg.de/~hermann/StoBe/.

(29) Becke, A. D. *Phys. Rev. A* **1988**, *38*, 3098.

(30) Perdew, J. P. *Phys. Rev. B* **1986**, *33*, 8822.

(31) Perdew, J. P.; Burke, K.; Ernzerhof, M. *Phys. Rev. Lett.* **1996**, *77*, 3865.

(32) Kutzelnigg, W.; Fleischer, U.; Schindler, M. *NMR*−*Basic Principles and Progress*; Springer-Verlag: Heidelberg, Germany, 1990.

(33) Pettersson, L. G. M.; Wahlgren, U.; Gropen, O. *J. Chem. Phys.* **1987**, *86*, 2176.

(34) Nakajima, R.; Stohr, J.; Idzerda, Y. U. *Phys. Rev. B* **1999**, *59*, 6421.

(35) Parent, P.; Laffon, C.; Mangeney, C.; Bournel, F.; Tronc, M. *J. Chem. Phys.* **2002**, *117*, 10842.

(36) Cavalleri, M.; Odelius, M.; Nordlund, D.; Nilsson, A.; Pettersson, L. G. M. *Phys. Chem. Chem. Phys.* **2005**, *7*, 2854.

(37) Schwegler, E.; Galli, G.; Gygi, F. *Phys. Rev. Lett.* **2000**, *84*, 2429.

(38) Hetenyi, B.; De Angelis, F.; Giannozzi, P.; Car, R. *J. Chem. Phys.* **2004**, *120*, 8632.

(39) Prendergrast, D.; Galli, G. *Phys. Rev. Lett.* **2006**, *96*, 215502.

(40) Sorenson, J. M.; Hura, G.; Glaeser, R. M.; Head-Gordon, T. *J. Chem. Phys.* **2000**, *113*, 9149.

(41) Odelius, M.; Cavalleri, M.; Nilsson, A.; Pettersson, L. G. M. *Phys. Rev. B* **2006**, *73*.

(42) The ice structure used in our XAS calculation was downloaded from http://sharepoint.cisat.jmu.edu/isat/klevicca/Web/VISM/VISM.htm.

(43) Eaves, J. D.; Loparo, J. J.; Fecko, C. J.; Roberts, S. T.; Tokmakoff, A.; Geissler, P. L. *Proc. Natl. Acad. Sci. U.S.A.* **2005**, *102*, 13019.

(44) Nyberg, M.; Odelius, M.; Nilsson, A.; Pettersson, L. G. M. *J. Chem. Phys.* **2003**, *119*, 12577.

(45) Cappa, C. D.; Smith, J. D.; Messer, B. M.; Cohen, R. C.; Saykally, R. J. *J. Phys. Chem. B* **2006**, *110*, 5301.